

Alpha-particle doorway states in ^{28}Si

Kenji Katori, Kohei Furuno, Takao Ooi, and Susumu Hanashima

Institute of Physics and Tandem Accelerator Center, The University of Tsukuba, Ibaraki 300-31, Japan

(Received 16 April 1979)

Excitation functions for the $^{12}\text{C}(^{16}\text{O}, ^{12}\text{C}_{g.s.})^{16}\text{O}$ reaction feeding the $0^+, 6.049$ -, $3^-, 6.131$ -, $2^+, 6.919$ -, $1^-, 7.117$ -, $4^+, 10.353$ -, and $4^+, 11.095$ -MeV states of ^{16}O have been measured at $\theta_{\text{lab}} = 7.0^\circ$ over the energy range $22.7 \leq E_{\text{c.m.}} \leq 37.7$ MeV in 86- or 173-keV steps. The Ericson-fluctuation type analysis was performed and nonfluctuating enhancements with a width of 700 keV are observed at $E_{\text{c.m.}} = 23.6, 24.6, 28.4$, and 32.2 MeV for the $0^+, 6.049$ - MeV states. The most probable total spins for the lowest three states are assigned to be $J^\pi = 14^+, 14^+$, and 15^- , respectively. These enhancements are strongly correlated to those for the $2^+, 6.919$ -MeV state, but anticorrelated to those for the $3^-, 6.131$ -MeV state. Model calculations based on Hauser-Feshbach and band-crossing theories were performed and none of them have succeeded to reproduce the data in a consistent way. Alpha-particle doorway states embedded in the high excitation of ^{28}Si (39–54 MeV) are indicative to describe these intermediate-structure resonances.

[NUCLEAR REACTIONS $^{12}\text{C}(^{16}\text{O}, ^{12}\text{C})^{16}\text{O}$; $E = 53$ –88 MeV, $\theta_{\text{lab}} = 5^\circ$ –16.5°; measured $\sigma(E, \theta)$, deduced resonances, J^π ; correlation analysis of fluctuations.]

I. INTRODUCTION

The subjects of resonant phenomena and intermediate structure in heavy ion scatterings and reactions have been recently of great interest and have been extensively studied both from theoretical and experimental points of view. At first, the $^{12}\text{C} + ^{12}\text{C}$ system was extensively investigated and successively the $^{12}\text{C} + ^{16}\text{O}$ system was attacked notably in the various exit channels below mainly $E_{\text{c.m.}} = 23$ MeV, since the narrow resonance was discovered at 19.7 MeV.¹ The recent reviews are provided in the literature.²⁻³

The most elaborate work on intermediate structure resonances in the inelastic scattering of ^{12}C on ^{16}O has been recently published by Malmin, Harris, and Paul⁴ who elucidated the physical situation in the energy region between 14 and 23 MeV. As conclusions, they indicated four important points and summarized them as follows: (1) The inelastic channels show a great deal of nonstatistical resonances of a width intermediate between Ericson fluctuations and ion-ion potential resonances. (2) Only a very few angular momenta in the incident channel contribute to the inelastic channels. Individual structures have unique spin assignments. (3) Inelastic channels dominate the structure of the observed resonances, both relatively and absolutely. (4) The emerging picture of at least the present resonances is that of eigenstates, which are populated through an L window or doorway and which are structurally only one or two steps removed from the entrance channel. Indications point toward alpha-particle exchange. Even though they took extensive data and made

various analyses on them, two contrasting mechanisms—one for the extended double-resonance model⁵⁻⁸ and the other for the resonant alpha-particle doorway-state model⁹⁻¹²—could not be decisively distinguished.

The further work which should be done in order to check their conclusions in the $^{12}\text{C} + ^{16}\text{O}$ system and to distinguish one model from the other would be (1) to extend the bombarding energy range to higher than 23 MeV in order to find other additional sequences of resonances and to confirm the rise and fall of resonant yields until reaching the continuum region, (2) to separate the $0^+, 6.049$ -MeV state from the $3^-, 6.131$ -MeV state and the $2^+, 6.919$ -MeV state from the $1^-, 7.117$ -MeV state in the final spectrum, and to measure the corresponding excitation functions, because these states have contrasting characters; i.e., the $0^+, 6.049$ -MeV state and the $2^+, 6.919$ -MeV state belong to the 4p-4h member of the deformed rotational band in ^{16}O , while the $3^-, 6.131$ -MeV state belongs to the 1p-1h state, and (3) to investigate a number of excitation functions for other different kinds of excited states in ^{16}O and ^{12}C .

In the present work, we investigated the $^{12}\text{C}(^{16}\text{O}, ^{12}\text{C}_{g.s.})^{16}\text{O}$ reaction to six excited states in ^{16}O . Detailed excitation functions to these states were measured at $\theta_{\text{lab}} = 7.0^\circ$ over a wide range of center-of-mass energies from 22.7 MeV to 37.7 MeV, corresponding to the excitations from 39.4 MeV to 54.4 MeV in ^{28}Si . Angular distributions for the 0^+ , 3^- , and 2^+ states were measured to determine the spins of the observed resonances.

If alpha-particle doorway states really exist at the high excitation of a composite nucleus, a good

choice of a system, an exit channel, a bombarding energy, and kinematics is essential to find them. The $^{12}\text{C} + ^{16}\text{O}$ system, like $^{16}\text{O} + ^{20}\text{Ne}$ is considered to be an easier system to allow an alpha particle to be attracted by each of two identical ^{12}C cores and to exchange it in a potential formed during the collision.¹⁰ If the alpha-exchange mechanism is dominant during the collision of ^{16}O and ^{12}C , the resonant alpha-transfer process will be able to be more sensitively observed in the excitation function for the transition to the 0^+ , 6.049-MeV state in ^{16}O in the $^{12}\text{C}(^{16}\text{O}, ^{12}\text{C})^{16}\text{O}^*$ reaction than for that to the ground state. This is because calculated spectroscopic factors ($^{16}\text{O} \rightarrow ^{12}\text{C} + \alpha$) are twice as large for the 0^+ , 6.049-MeV state as for the ground state [$S(0^+, 6.049 \text{ MeV})/S(\text{g.s.}) = 0.679/0.300$].¹³ In addition, the rise in the differential cross section at backward angles for the 0^+ , 6.049-MeV state in the $^{12}\text{C}(^{16}\text{O}, ^{16}\text{O})^{12}\text{C}$ scattering is observed and considered to be due to the population of the 0^+ , 6.049-MeV state not by inelastic scattering but by alpha transfer since the monopole strength is small.

On the other hand, for the higher excitations in the p - and sd -shell mass nuclei, multimolecular structures with the linear chain configuration were proposed by Horiuchi, Ikeda, and Suzuki.¹⁴ The bombarding energies, where intermediate structure resonances appear, correspond to those predicted by them, and thus the resonant alpha-exchange process will be expected to occur through eigenstates with more complex alpha configurations in the decays to such low-lying alpha-cluster states if they are kinematically allowed to be populated during the collision.

Reports of the present work have been partly presented elsewhere.¹⁵

II. EXPERIMENTAL PROCEDURE

An $^{16}\text{O}^{5+,6+,7+}$ beam was delivered by the 12 UD Pelletron Tandem Accelerator at the University of Tsukuba.¹⁶

The outgoing $^{12}\text{C}^{6+}$ particles were momentum-analyzed by an ESP-90 magnetic spectrograph¹⁷ and detected using two 47 mm silicon position-sensitive detectors placed in the focal plane. One detector covered particles for the transitions to the 0^+ , 3^- , 2^+ , and 1^- states of ^{16}O and the other covered ^{12}C particles for the 4^+ (10.353 MeV) and 4^+ (11.095 MeV) states. For data acquisition, conventional analog dividers were used to get position signals gated by the energy signals of $^{12}\text{C}^{6+}$ particles. In half of the runs, the energy and the energy-times-position signals were stored on-line in PDP 11/40 and 11/50 computers. Two-dimensional analyses were made off-line to get the momentum spectrum of $^{12}\text{C}^{6+}$ particles.

The actual overall energy resolution obtained for ^{12}C was about 70 keV for a self-supporting carbon natural foil $29 \mu\text{g}/\text{cm}^2$ thick. This energy resolution is necessary and sufficient to separate the transitions to the 0^+ , 6.049-MeV state from the 3^- , 6.131-MeV state without losing counting rates. Spectra are shown in Figs. 1(a) and 1(b). The target thickness used was measured by the energy-loss method using an ESP-90 spectrograph with an ^{241}Am α source just before and after each run to check carbon buildup. No significant indication of it was found. A solid angle of 0.94 msr was usually used, which corresponded to $\Delta\theta_{\text{lab}} = \pm 0.72^\circ$ ($\Delta\theta_{\text{c.m.}} = \pm 1.5^\circ$). Zero degree checks were made before and after each run in the angular distribution measurements to confirm the beam direction with respect to the scale of the magnet since no beam collimators were used along the beam line. One-point position check at the target and good

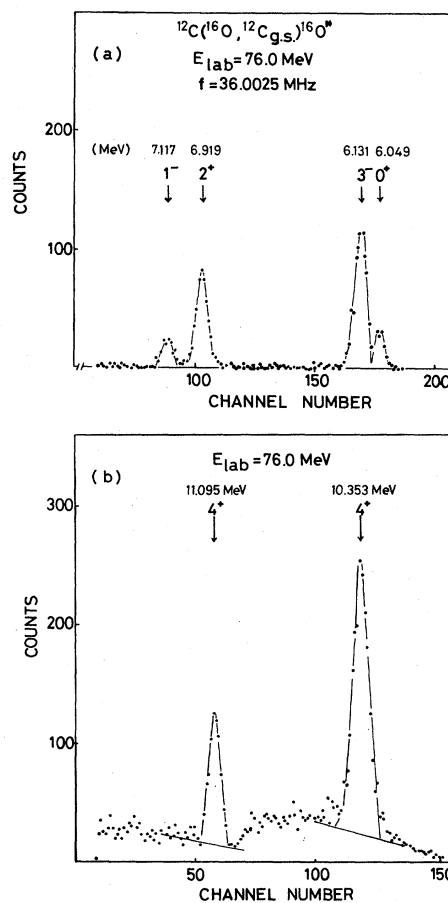


FIG. 1. Momentum spectra of the $^{12}\text{C}^{6+}$ particles at $E_{\text{c.m.}} = 32.57 \text{ MeV}$ ($E_{\text{lab}} = 76.0 \text{ MeV}$) in the $^{12}\text{C}(^{16}\text{O}, ^{12}\text{C})^{16}\text{O}$ reaction measured at $\theta_{\text{lab}} = 7.0^\circ$: (a) for the 0^+ , 6.05-, 3^- , 6.13-, 2^+ , 6.92-, and 1^- , 7.12- MeV states of ^{16}O , (b) for the 4^+ , 10.35- and 4^+ , 11.10-MeV states of ^{16}O .

tuning of the beam direction could set the beam within $\theta_{\text{lab}} \leq 0.2^\circ$ for each run as this is important for obtaining correct large- L values.

The absolute cross section was estimated to have an uncertainty of 20% which includes uncertainties of the charge collection, target thickness, and detection efficiency.

The excitation functions for the $^{12}\text{C}(^{16}\text{O}, ^{12}\text{C}_{g.s.})^{16}\text{O}^*$ reaction feeding the six states— 0^+ , 6.049, 3^- , 6.131, 2^+ , 6.919, 1^- , 7.117, 4^+ , 10.353, and 4^+ , 11.095 MeV—of $^{16}\text{O}^*$ were measured at $\theta_{\text{lab}} = 7.0^\circ$. The angle of $\theta_{\text{lab}} = 7.0^\circ$ for the excitation function measurements is chosen because this is the position of the first maximum of $|P_L(\cos\theta)|^2$ at $\theta_{\text{c.m.}} \sim 15^\circ$ for $L = 12-17$ in the region of $20 \leq E_{\text{c.m.}} \leq 40$ MeV. If one L value dominates, a peak will be found in the cross section at this angle.

For the four states (0^+ , 3^- , 2^+ , and 1^-), measurements were made from $E_{\text{lab}} = 53.0$ to 77.0 MeV ($22.7 \leq E_{\text{c.m.}} \leq 33.0$ MeV) in steps of 0.2 MeV (86 keV in c.m. system) and from $E_{\text{lab}} = 77.0$ to 88.0 MeV ($33.0 \leq E_{\text{c.m.}} \leq 37.7$ MeV) in steps of 0.4 MeV (173 keV in c.m. system), but the 0^+ and 3^- states were not separated in the higher energy region (77–88 MeV).

For the two 4^+ states (10.353- and 11.095-MeV states), measurements were made from $E_{\text{lab}} = 62.4$ to 77.0 MeV and from $E_{\text{lab}} = 65.2$ to 77.0 MeV, respectively, in steps of 0.2 MeV and from 77.0 to 88.0 MeV in steps of 0.4 MeV.

Angular distributions were measured at $E_{\text{c.m.}} = 23.7$, 24.3, and 28.2 MeV on the enhanced cross sections and at 25.2 MeV between the enhanced peaks. A preliminary angular distribution was measured at $E_{\text{c.m.}} = 32.2$ MeV. The angular distributions were taken from $\theta_{\text{lab}} = 5.0^\circ$ to 16.5° in steps of $\Delta\theta_{\text{lab}} = 0.5^\circ$ with the angular resolution of $\Delta\theta_{\text{lab}} = \pm 0.58^\circ$ ($\Delta\theta_{\text{c.m.}} \sim \pm 1.1^\circ$) for the 0^+ , 3^- , and 2^+ states and also for the 1^- state at $E_{\text{c.m.}} = 25.2$ and 28.2 MeV. The angular range of measurements at the backward angles was limited by the pole pieces of the magnet if the 0^+ and 3^- peaks are to be resolved.

III. EXPERIMENTAL RESULTS

Experimental results are presented in turn for the transitions to the six states the 3^- , 0^+ , 2^+ , 1^- , 4^+ (10.353 MeV), and 4^+ (11.095 MeV) states in ^{16}O . Discussion of the excitation functions for the 0^+ , 6.049- and 3^- , 6.131-MeV states is made in the previous paper.¹⁵ New data taken after this publication are presented in this section.

The 3^- , 6.131-MeV state. We extended the excitation function measurements from $E_{\text{c.m.}} = 33.0$ to 37.7 MeV for the unseparated 0^+ and 3^- states as

shown in Fig. 2. In this bombarding energy region the differential cross section for the 0^+ state is assumed to be reduced rapidly, and the contribution to the cross section for the 3^- state is less than 10%. An enhancement of the cross section is newly observed around 35.2 MeV. Except for the large peak around 30 MeV, the envelope of peaks gradually decreases with the bombarding energy.

The excitation function at $\theta_{\text{lab}} = 4.0^\circ$ measured by Shapira *et al.*¹⁸ is in good agreement with our data in the energy region of $22.7 \text{ MeV} \leq E_{\text{c.m.}} \leq 29.2$ MeV, although transitions to the 0^+ and 3^- states were not separated in their data.

The data for the unseparated 0^+ and 3^- states

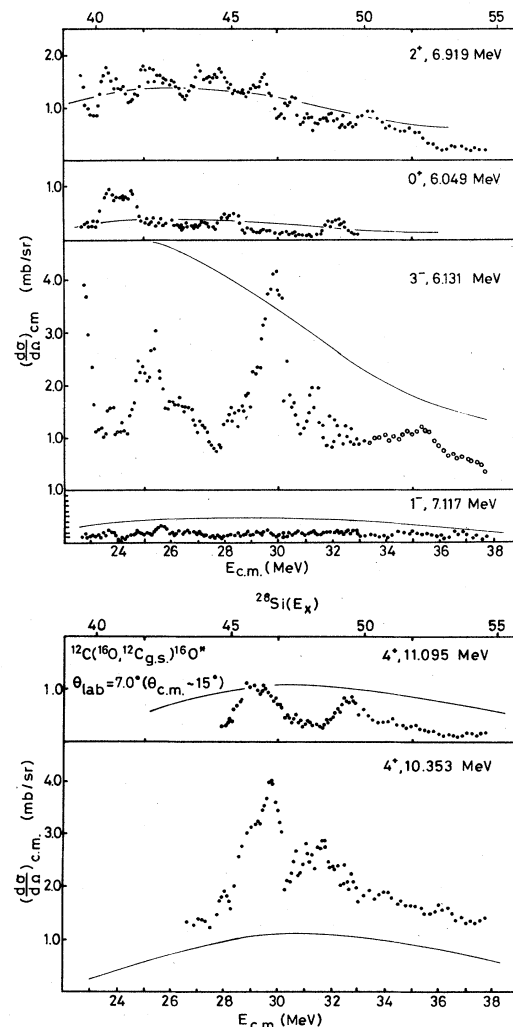


FIG. 2. Excitation functions in the transitions to the 1^- , 7.12-, 3^- , 6.13-, 0^+ , 6.05-, 2^+ , 6.92-, 4^+ , 10.35-, and 4^+ , 11.10-MeV states of ^{16}O measured at $\theta_{\text{lab}} = 7.0^\circ$ in the $^{12}\text{C}(^{16}\text{O}, ^{12}\text{C})^{16}\text{O}$ reaction. Open circles for the 3^- state indicate the sum of the cross sections for the 0^+ and 3^- states. Curves are results of Hauser-Feshbach calculations. See text in Sec. VIA for explanation.

measured by Malmin, Harris, and Paul⁴ at $\bar{\theta}_{c.m.} = 165^\circ$ in the energy region from 14 MeV to 24 MeV are also in good agreement with our data in the overlapping energy region. The relative peak heights of the two doublets appear reversed in the lower energy region. This feature may reveal channel-coupling effects between incoming and outgoing channels which cause a change in the relative intensity of the doublet with the bombarding energy.

The 0^+ , 6.049-MeV state. The total $0^+ - 0^+$ pair transition probability was measured by Malmin, Kahn, and Paul¹⁹ in the energy region from $19 \leq E_{c.m.} \leq 24$ MeV. Good correspondence with our data for the excitation function is observed in the overlapping energy region, especially the enhancement at $E_{c.m.} = 23.7$ MeV.

If the enhancement at 20.57 MeV is assumed to be due to the resonance with the definite spin of $J^\pi = 13^-$, which is suggested by Malmin, Kahn, and Paul,¹⁹ the band formation for the 0^+ , 6.049-MeV state ($J^\pi = 13^-, 14^+, 15^-,$ and 16^+ at energies of 20.57, 24.0, 27.5, and 31.5 MeV) follows the $J(J+1)$ trajectory quite well and can be further extended to the energy region of the fusion barrier in the incident channel. In fact, the spin assignment of $J^\pi = 13^-$ is confirmed by the good fitting of $|P_{13}(\cos\theta)|^2$ to their data taken at 20.5 MeV for the unseparated 0^+ and 3^- states, if one assumes that the main contribution to this resonance is from the 0^+ state between 140° and 172° .⁴

The doublet structure of the enhancements is also found in the energy region measured, although the reason for the occurrence of the doublets has not yet been explained. In the excitation function for the unseparated 3^- and 0^+ states, the doublet structure at $E_{c.m.} = 20.5$ MeV is also enhanced.⁴ The data taken by Shapira *et al.* at $\theta_{lab} = 4.0^\circ$ for the unseparated 3^- and 0^+ states do not show any sign of the doublet.¹⁸ However, this is understandable since the Legendre polynomials of $|P_L(\cos\theta)|^2$ have a minimum value at $\theta_{c.m.} \sim 8.0^\circ$ for L around 14.

The 2^+ , 6.919-MeV state. Although the 2^+ , 6.919-MeV state belongs to the same deformed rotational band as the 0^+ , 6.049-MeV state, the continuous part of the differential cross section has a larger yield than that for the 0^+ , 6.049-MeV state and less fluctuations are observed at $\theta_{lab} = 7.0^\circ$, although some of peaks correspond to the enhancements of the yields for the 0^+ state.

The excitation function measured at $\bar{\theta}_{c.m.} = 165^\circ$ by Malmin, Harris, and Paul⁴ for the unseparated 2^+ and 1^- states shows good agreement with our data in the energy region between 22.7 and 24 MeV. The excitation function measured at $\theta_{lab} = 4.0^\circ$ by Shapira *et al.*¹⁸ for the 2^+ state is in good correspondence with our data in the energy region be-

tween 22.7 and 29.2 MeV. In addition, the angular distribution at $E_{c.m.} = 25.54$ MeV is in good agreement with our data at $E_{c.m.} = 25.2$ MeV.

The 1^- , 7.117 state. The excitation function at $\theta_{lab} = 7.0^\circ$ is observed to be small and shows no strong fluctuations in the present bombarding energy region similar to that measured at $\theta_{lab} = 4.0^\circ$.¹⁸ However, the angular distributions at $E_{c.m.} = 28.2$ and 25.2 MeV show strong oscillations.

The 4^+ , 10.353-MeV and 4^+ , 11.095-MeV states. The excitation function for the 4^+ , 10.353-MeV state at $\theta_{lab} = 7.0^\circ$ shows a strong enhancement around 30 MeV and the yield gradually decreases at energies higher than 30 MeV. On the other hand, the excitation function for the 4^+ , 11.095-MeV state shows a rather smooth change with the bombarding energy and the yield gradually decreases. The energies at the enhancements of the yields for the 4^+ , 10.353-MeV state do not correspond to those for the 4^+ , 11.095-MeV state. The relative yield of the two 4^+ states at $E_{c.m.} = 37$ MeV, where both excitation functions become smooth, is about 20 times larger than the ratio of the α widths $\Gamma_{\alpha_0}(11.10)/\Gamma_{\alpha_0}(10.35) = 0.28$ keV/27 keV ~ 0.01 .²⁰ The ($^{16}\text{O}, ^{12}\text{C}$) reaction preferably populates the 4^+ , 11.095-MeV and 4^+ , 10.353-MeV states in the same ratio as the ($^6\text{Li}, d$) reaction.²¹

Within the 70 keV energy resolution in the spectrum, few states around 10.353-MeV and 11.095-MeV excitation in ^{16}O contribute to the excitation functions. It is inevitable that an ambiguity in subtracting the continuous contribution in the momentum spectrum causes an uncertainty larger than that for four low-lying 0^+ , 3^- , 2^+ , and 1^- states. The continuous part usually contributes less than 10% for the 4^+ , 10.353-MeV state and 20% for the 4^+ , 11.095-MeV state.

IV. THE ERICSON FLUCTUATION ANALYSES OF EXCITATION FUNCTIONS

In this section, we analyze the data, assuming that fluctuations in the excitation functions are due to many overlapping resonances with statistically random phases. We give the results of Ericson fluctuation type analyses²² of the measured excitation functions.

The energy-dependent averaged cross section is defined by

$$\langle \sigma(E_i) \rangle_N = \frac{1}{N} \sum_{j=i-N/2}^{i+N/2} \sigma(E_j),$$

where N is the number of ΔE steps in the averaging interval I . Using this averaged cross section, the deviation function $D(E)$, the autocorrelation function $R_{\alpha\alpha}(\epsilon)$, and the normalized cross-correlation function $C_{\alpha\alpha}(\epsilon)$ are defined as follows:

$$D(E) = \sigma(E)/\langle\sigma(E)\rangle - 1, \quad R_{\alpha\alpha}(\epsilon) = \langle(\sigma_{\alpha}(E)/\langle\sigma_{\alpha}(E)\rangle - 1)(\sigma_{\alpha}(E+\epsilon)/\langle\sigma_{\alpha}(E+\epsilon)\rangle - 1)\rangle,$$

and

$$C_{\alpha\alpha}(\epsilon) = \langle(\sigma_{\alpha}(E)/\langle\sigma_{\alpha}(E)\rangle - 1)(\sigma_{\alpha}(E+\epsilon)/\langle\sigma_{\alpha}(E+\epsilon)\rangle - 1)\rangle/[R_{\alpha\alpha}(0)R_{\alpha'\alpha'}(0)]^{1/2}.$$

The optimum averaging energy interval was determined from the autocorrelation function, where N was varied in order that the coherence width Γ and the autocorrelation function coefficient $R_{\alpha\alpha}(0)$ attain their plateau values.²³ In the present case, the averaging energy interval I of 1.81 MeV or 1.87 MeV (c.m. system) was chosen. This value is large enough to define a meaningful averaged cross section, but small enough to follow the intermediate structure evident in the data.

A. Autocorrelation functions

The autocorrelation functions of the excitation functions for the 0^+ , 3^- , 2^+ , and 1^- states are shown in Fig. 3(a) for the energy region between 22.71 and 33.0 MeV. The Lorentzian form $\Gamma^2/$

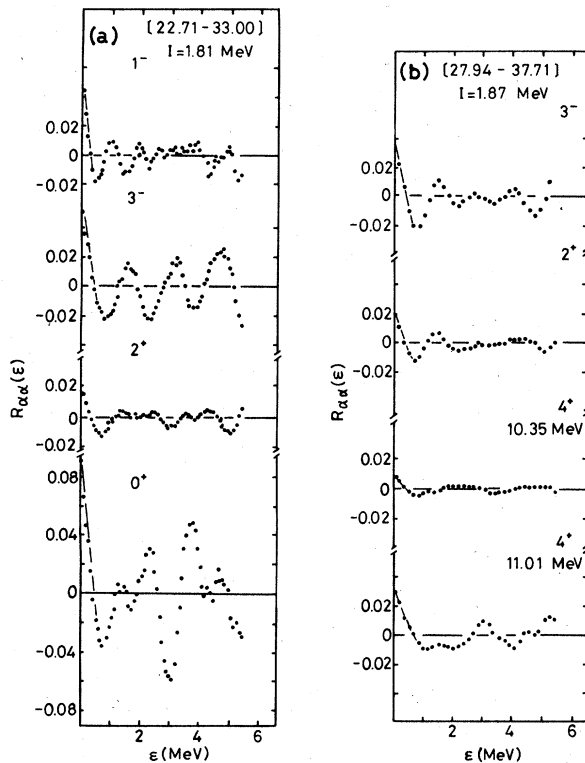


FIG. 3. The autocorrelation functions of the excitation functions: (a) for the 0^+ , 2^+ , 3^- , and 1^- states for the averaging energy interval of 1.81 MeV in the energy range from 22.71 to 33.00 MeV, (b) for the 2^+ , 3^- , 4^+ , 10.35- and 4^+ , 11.10-MeV states for the averaging energy interval of 1.87 MeV in the energy range from 27.94 to 37.71 MeV.

$(\Gamma^2 + \epsilon^2)$ is found for $\epsilon < 0.5$ MeV, and thereafter periodic oscillations are dominant for all four states especially for the 3^- state. These oscillations are too regular to be caused by finite-range-of-data effects for large values of ϵ , and also the ratio of the range to ΔE is too large for this interpretation.²⁴ The coherence widths for the four states range from 150 keV to 200 keV, which are about 4 times smaller than the width of ~ 700 keV obtained by the resonance analysis for the 0^+ state as shown in the next section.

For the 3^- state, the periodicity of ~ 1.6 MeV is maintained with no evident reduction in amplitude up to ϵ value of 5 MeV. Kolata *et al.*²⁵ reported a periodicity of ~ 725 keV in the total fusion cross section in the energy region between 17 and 28 MeV. This reduction of the periodicity to half its value is understandable if one considers that the correlation functions for the 3^- and 0^+ states have an opposite phase and an almost equal period over this energy region.

For the 0^+ state, a doublet separation of ~ 1.2 MeV is found with a repetition separation of ~ 3.6 MeV. Obviously, the regular enhancements at $E_{\text{c.m.}} = 23.7, 24.7, 27.0, 28.2, 30.5,$ and 32.2 MeV shown in Fig. 2. are responsible for the regular periodicity in the autocorrelation function.

For the 2^+ state, the autocorrelation function [Fig. 3(a)] is similar to that for the 0^+ state with a slightly damped amplitude. The similarity of the periodicity can be regarded as coming from the excitation function decaying to the same member of the deformed rotational band of ^{16}O .

For the 1^- state, the periodicity of ~ 1 MeV is maintained with the gradual damping of the amplitude up to $\epsilon \sim 5$ MeV.

The autocorrelation function coefficients $R_{\alpha\alpha}(0)$ in the higher bombarding energy region between 27.94 and 37.71 MeV shown in Table I are smaller than those in the lower energy region between 22.71 and 33.00 MeV for the 2^+ and 3^- states.

This indicates that the previously found anomalous enhancements due to the intermediate-structure resonance gradually damp in the region from the energy of the Coulomb barrier plus the centrifugal barrier to about four times energy of the Coulomb barrier, finally giving the continuous cross section, and similarly for the autocorrelation function coefficients for two channels.

For the 4^+ , 10.35-MeV state and for the 4^+ , 11.10-MeV state, the autocorrelation functions

TABLE I. The coherence widths, the percentages of the noncompound reaction, autocorrelation function coefficients, and cross-correlation function coefficients obtained in the Ericson fluctuation analyses. The energy range analyzed and the interval of the moving average are indicated. In deducing the percentage of the noncompound reaction, $N_{\text{eff}}=1$ is assumed. The uncertainties indicated come from the uncertainties of a choice of the averaging interval.

(a) The coherence width Γ and the percentage of the noncompound reaction Y_D				
State	(22.71–33.00 MeV)		(27.94–37.71 MeV)	
	Γ (keV)	Y_D (%)	Γ (keV)	Y_D (%)
0^+ , 6.05–MeV	165 ± 20	95 ± 1		
2^+ , 6.92–MeV	141 ± 15	99 ± 1	210 ± 30	99 ± 1
3^- , 6.13–MeV	164 ± 20	97 ± 1	230 ± 30	98 ± 1
1^- , 7.12–MeV	109 ± 15	98 ± 1	158 ± 30	98 ± 1
4^+ , 10.35–MeV			195 ± 30	99 ± 1
4^+ , 11.10–MeV			274 ± 50	98 ± 1

(b) The autocorrelation and cross-correlation function coefficients $R_{\alpha\alpha}(0)$ and $C_{\alpha\alpha'}(0)$ (22.71–33.00 MeV), $I=1.81$ MeV				
	0^+ , 6.05 MeV	2^+ , 6.92 MeV	3^- , 6.13 MeV	1^- , 7.12 MeV
0^+ , 6.05 MeV	0.094 ± 0.018	0.151	-0.058	0.099
2^+ , 6.92 MeV		0.022 ± 0.002	-0.142	0.226
3^- , 6.13 MeV			0.052 ± 0.012	0.235
1^- , 7.12 MeV				0.045 ± 0.004

(c) The autocorrelation and cross-correlation function coefficients $R_{\alpha\alpha}(0)$ and $C_{\alpha\alpha'}(0)$ (27.94–37.71 MeV), $I=1.87$ MeV				
	3^- , 6.13 MeV	2^+ , 6.92 MeV	4^+ , 10.35 MeV	4^+ , 11.10 MeV
3^- , 6.13 MeV	0.032 ± 0.008	-0.102	0.524	0.186
2^+ , 6.92 MeV		0.019 ± 0.003	-0.072	0.025
4^+ , 10.35 MeV			0.008 ± 0.002	0.149
4^+ , 11.10 MeV				0.030 ± 0.012

are quite different from those for the other four states [Fig. 3(b)].

The autocorrelation function coefficient $R_{\alpha\alpha}(0)$ is proportional to $(1/N_{\text{eff}})[1 - \langle \langle \sigma \rangle_{D_I} / \langle \sigma \rangle \rangle^2]$, following Ericson's prescription. For the 0^+ state, N_{eff} is unity for all angles, and hence $R_{\alpha\alpha}(0) = 0.0935$ gives $Y_D = \langle \langle \sigma \rangle_{D_I} / \langle \sigma \rangle \rangle = 0.952$. This value of 95% direct component is far from reality in the case when the intensity is localized on regularly spaced resonances within the width of ~ 700 keV and at the energy interval of ~ 3.6 MeV. For the 2^+ and 3^- states, similar values of the direct component can be extracted assuming reasonable values of N_{eff} in the range $1 \leq N_{\text{eff}} \leq (I_B + 1)$.

The results obtained by Ericson fluctuation analyses are summarized in Table I.

B. Cross-correlation functions

The cross-correlation functions were taken for the channels between the 0^+ and 2^+ states, the 0^+ and 3^- states, the 2^+ and 3^- states, the 3^- and 1^- states, the 0^+ and 1^- states, and the 2^+ and 1^- states in the energy region between 22.71 and 33.00 MeV. The two-channel cross-correlation functions for the 0^+ and 3^- states and the 2^+ and 3^-

states are completely out of phase, whereas those for the channels between the 0^+ and 2^+ states and the 3^- and 1^- states are in phase. The cross-correlation function coefficients at $\epsilon = 0$ have opposite sign for the channels between the 0^+ and 3^- states and the 2^+ and 3^- states as shown in Table I.

In the higher energy region between 27.94 and 37.71 MeV, the cross-correlation function coefficient between the 2^+ and 3^- states is still negative, while that between the 3^- and 4^+ , 10.35-MeV states is positive.

To summarize this section, the Ericson fluctuation analyses failed to describe any of the features of the excitation function for the six states in ^{16}O . The random-phase assumption between compound states does not hold in this bombarding energy region, but the states with one or two dominant and definite J 's may be localized and the phases of the partial decay widths of these states in the different decay channels may be correlated.

C. Deviation functions

The deviation function for the 0^+ , 6.05-MeV state shown in Fig. 4 clearly shows peaks at $E_{\text{c.m.}} = 23.7, 24.7, 27.0, 28.2, 30.5, \text{ and } 32.2$ MeV as

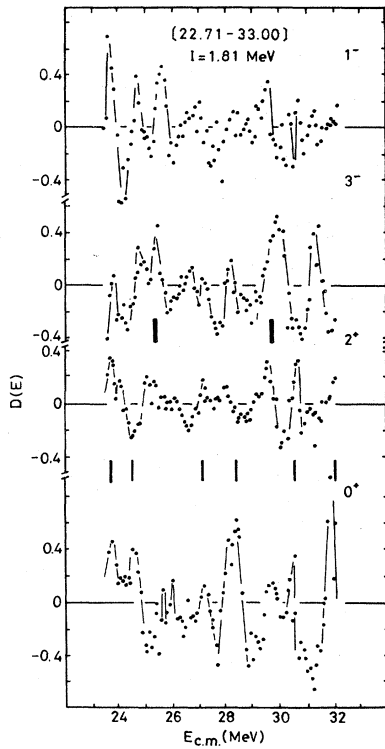


FIG. 4. The deviation functions for the 0^+ , 2^+ , 3^- , and 1^- states in the energy region from 22.71 to 33.00 MeV.

seen at the energies in the excitation function.

In the deviation function for the 2^+ state, the lower energy peak of the doublet for the 0^+ state corresponds quite well to the lower energy peak for the 2^+ state, whereas the higher energy peak of the doublet for the 0^+ state corresponds to the minimum after the first zero crossing point for the 2^+ state. It is noteworthy that the peaks for the 2^+ state correspond to the peaks for the 3^- state, and their intensities indicate the moderately strong coupling between those two channels. Alternatively, the peaks for the 3^- state are weakly correlated with the peaks for the 0^+ and 2^+ states.

For the excitation functions for the 2^+ , 6.92-MeV

and $3^-(0^+)$ states measured at $\theta_{\text{lab}} = 4.0^\circ$, Shapira *et al.*¹⁸ pointed out the good correspondence of peaks between those two channels around 25 MeV.

For the 4^+ , 11.10-MeV state, the position and distribution of the peaks do not resemble those for other states.

V. THE S-MATRIX ANALYSES OF ANGULAR DISTRIBUTIONS

In this section, we start from an assumption opposite to that in the previous section, i.e., the enhancements observed in the excitation functions are due to resonances. In this case the angular distribution taken on a resonance would show characteristic features, since it should have single definite spin and parity.

For determining the total spin of the resonances, angular distributions were measured for the 0^+ , 6.05-MeV, 3^- , 6.13-MeV, and 2^+ , 6.92-MeV states at $E_{\text{c.m.}} = 23.7, 24.3, 25.2, 28.2,$ and 32.2 MeV and for the 1^- , 7.12-MeV state at $E_{\text{c.m.}} = 25.2$ and 28.2 MeV.

By the fitting of the Legendre polynomials $|P_J(\cos\theta)|^2$ to the angular distribution for the 0^+ state, the total spins were determined. Single definite spins are assigned to the resonances at $E_{\text{c.m.}} = 23.7, 24.3,$ and 28.2 MeV and the most probable spin values are $J^\pi = 14^+, 14^+,$ and 15^- , respectively. The preliminary angular distributions at $E_{\text{c.m.}} = 32.2$ MeV indicates the total spin to be $J^\pi = 16^+$.

At $E_{\text{c.m.}} = 25.2$ MeV off-resonance, the angular distribution cannot be fitted by a single Legendre polynomial. However, a good fit was obtained with $J^\pi = 14^+$ and 16^+ interfering with equal weight and opposite sign.

To confirm these spin assignments, the S-matrix analyses of the angular distributions for the 3^- , 6.13-MeV and 2^+ , 6.92-MeV states were performed. If all relevant states have zero spin except the final state of spin I_B and the intermediate state of spin J , the angular distributions can be simplified to give

$$d\sigma/d\Omega = \pi\lambda^2 \sum_{m_B} \left| \sum_{J, L_f} (2J+1)^{1/2} (L_f - m_B I_B m_B | J0) S_{I_B L_f, 0 J}^J Y_{L_f}^{m_B}(\Omega) \right|^2.$$

In the case of a single J value, the angular distribution for the 2^+ state monotonically decreases for $L_f = J \pm 2$. The only oscillatory angular distribution appears for $L_f = J$. The angular distribution for the 3^- state also monotonically decreases for $L_f = J \pm 3$, while the angular distributions show os-

cillations for $L_f = J \pm 1$. Since the largest transmission coefficient appears for the smallest L_f , the angular distribution predicted in the S-matrix expression favors the stretching schemes with $L_f = J - 2$ and $L_f = J - 3$ for the 2^+ and 3^- states, respectively, and hence should show a monotonic

decrease with angle.

Contrary to this prediction, all the measured angular distributions except that for the 3^- state at $E_{c.m.} = 23.7$ MeV show strongly oscillatory distributions. These oscillatory angular distributions were generated by increasing the amplitude of the matrix element with $L_f = J$ or $L_f = J - 1$ against that with $L_f = J - 2$ or $L_f = J - 3$. By adjusting the mixing ratio of the matrix elements for different L_f in the exit channel, good fits were able to be obtained as shown in Fig. 5. For example, the mixing ratio of $S_{2,14,0,14}^{14}/S_{2,12,0,14}^{14} = 0.75$ was the best fit one for the 2^+ , 6.92-MeV state at $E_{c.m.} = 23.7$ MeV, which was twice as large as the value expected by transmission coefficients.

The quality of the fit to the oscillations in the angular distributions for the 3^- and 2^+ states gives a good measure of the accuracy of the J values. Thus, the total spins for the resonances at $E_{c.m.} = 23.7$, 24.3, and 28.2 MeV were confirmed to be $J^\pi = 14^+$, 14^+ , and 15^- , respectively. Again, at $E_{c.m.} = 25.2$ MeV the mixing of the $J^\pi = 14^+$ and 16^+ components must be taken into account to fit the data and this supports the spin determination made for the 0^+ state.

For the 1^- state at $E_{c.m.} = 28.2$ MeV, the fit is quite good at supporting the spin assignment of $J^\pi = 15^-$.

Using these values for the total spins of the resonances, the excitation functions for the 0^+ state were fitted by the Breit-Wigner resonance formula

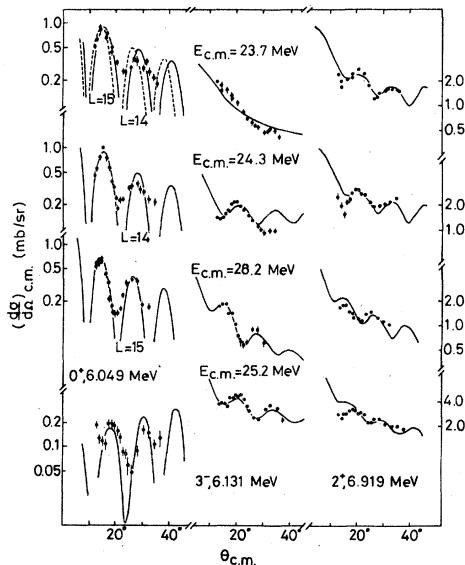


FIG. 5. The angular distributions for the 0^+ , 2^+ , 3^- states at $E_{c.m.} = 23.7$, 24.3, 25.2, and 28.2 MeV with the curves fitted in the S -matrix expression. For the 3^- and 2^+ states, see the right-side scale for the differential cross sections.

la and the resonance parameters were extracted.¹⁵ Obviously, the fit for the two-level formula is better than for the one-level formula as shown in Fig. 6. This fact confirms that the resonances at $E_{c.m.} = 23.6$ and 24.6 MeV and at $E_{c.m.} = 27.0$ and 28.4 MeV are of the same total spin, respectively. The resonance parameters extracted are tabulated in Table II.

As a summary of this section, the states with one or two definite dominant total spins J 's appear to bunch within the localized energy region to form resonances.

VI. TWO MODEL CALCULATIONS

In the present section, the measured differential cross sections for the six states of ^{16}O is compared as a function of the bombarding energy to the calculated cross sections based on the Hauser-Feshbach and the band-crossing theories.

A. The Hauser-Feshbach theory calculation

The calculations based on the Hauser-Feshbach theory²⁶ were made as an extension from those made at lower bombarding energies.²⁷ Denominators $G(J)$ are calculated at $E_{c.m.} = 30$ MeV, and the interpolation has been made between $E_{c.m.} = 24$ and 30 MeV by using energy-dependent parameters.²⁸ Transmission coefficients for the numerators are calculated using shallow⁴ and deep²⁹ potential parameters and the results are shown in Figs. 2 and 7.

The calculated bombarding energy dependence of the cross sections for all states reproduces the energy-averaged cross sections at $\theta_{c.m.} = 15^\circ$ quite well as shown in Fig. 2. An increase at the lower energy and a gradual decrease at higher energies are able to reproduce fairly well the cross sections for the 0^+ , 2^+ , 3^- , 4^+ , 10.35-MeV and 4^+ , 11.10-MeV states.

Adding data taken at $\bar{\theta}_{c.m.} = 165^\circ$ for the unseparated 0^+ and 3^- states measured by Malmin, Harris, and Paul⁴ in the lower energy range to the present one for the 3^- state, one can draw an envelope with a rapid rise from 17 to 22 MeV and a slow fall from 23 to 37 MeV; in this energy region the peaks of the strongly localized enhancements

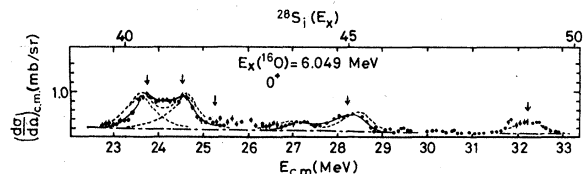


FIG. 6. The excitation function for the 0^+ , 6.05-MeV state and the fits by the Breit-Wigner one- (dotted line) and two- (full line) level resonance formula.

TABLE II. Resonance parameters—resonance energies, total spins, total widths, and products of elastic and inelastic partial widths—which were extracted from the fit shown in Fig. 6.

E_R (MeV)	J^π	Γ (keV)	$\Gamma_e \Gamma_{c'}$ (keV ²)
23.60	14^+	640	1640
24.60	14^+	640	1680
27.00	(15^-)	680	480
28.40	15^-	680	1130
32.20	(16^+)	720	750

are included.

Around $E_{c.m.} = 30$ MeV, another sort of anomalous enhancement with an width of ~ 1 MeV may be observed not only in the excitation functions of the differential cross sections for the 3^- and 4^+ states at $\theta_{c.m.} = 15^\circ$, but also in the excitation functions of the double cross sections for the $4^+(10.35\text{-MeV})$ and $6^+(14.82\text{-MeV})$ states at $\theta_{lab}^1 = 30^\circ$ and $\theta_{lab}^2 = 30^\circ$.³⁰ This anomalous phenomenon remains an open question to be investigated.

For the absolute cross section, the calculated

values for the 3^- , 1^- , and 4^+ , 11.10-MeV states are larger than the experimental values, whereas those for the 0^+ , 2^+ , and 4^+ , 10.35-MeV states are almost equal to or smaller than the experimental values. This important difference will be explained later.

The calculated angular distributions reproduce the data only for the 0^+ state at $E_{c.m.} = 23.7$ and 24.3 MeV as shown in Fig. 7. The angular distribution at the higher energies appears to shift a little toward the forward angle. At $E_{c.m.} = 25.2$ MeV, where the energy region is considered to be in the many-level-overlapping energy region so that the statistical assumption is valid, the calculated curves are completely out of phase with the data. For the 2^+ and 3^- states, the calculated curves show a smooth decrease, while the experimental data are strongly oscillatory. Thus, in contrast to the S-matrix analyses, the Hauser-Feshbach theory can not reproduce the data for the 0^+ , 2^+ , and 3^- states as a whole.

This suggests that the cross section is not due to the contributions of many J 's with random phases, but rather comes from a narrow band of J 's whose contributions combine constructively; we call this the J -narrowing effect.

To summarize, the general trend of the excitation functions for the six states can be fairly well described by the Hauser-Feshbach theory. However, the intermediate-resonance structures and the angular distributions for the 2^+ and 3^- states cannot be described in this way. Thus, it is difficult to attribute the reaction mechanism to the statistical process.

B. The band-crossing model calculation

The numerical calculations of the excitation functions for the transitions to the 0^+ , 6.05-MeV, 2^+ , 6.92-MeV, and 4^+ , 10.35-MeV states of ^{16}O in the $^{12}\text{C}(^{16}\text{O}, ^{12}\text{C})^{16}\text{O}^*$ reaction have been tried here by applying a band-crossing model.^{7,31} Many calculations for molecular resonances were performed by Matsuse, Kondo, and Abe³¹ for the transitions to the $2^+(4.44$ MeV in $^{12}\text{C})$ and $3^-(6.13$ MeV in $^{16}\text{O})$ states in the $^{12}\text{C}(^{16}\text{O}, ^{16}\text{O}^*)^{12}\text{C}$ reactions. They found that the experimental excitation functions of the differential and angle-integrated cross sections to the $2^+(4.44$ MeV in $^{12}\text{C})$ and $3^-(6.13$ MeV in $^{16}\text{O})$ and of the elastic scattering are well reproduced in the energy region below $E_{c.m.} = 26$ MeV in the band-crossing model calculation.

We have extended similar calculations to a higher energy region up to 34 MeV with more channels.

The channels coupled together are increased to seven, and grouped into three sections: (i) $^{12}\text{C}_{g.s.} + ^{16}\text{O}_{g.s.}$ and $^{12}\text{C}(2^+, 4.44$ MeV) + $^{16}\text{O}_{g.s.}$, (ii) $^{12}\text{C}_{g.s.}$

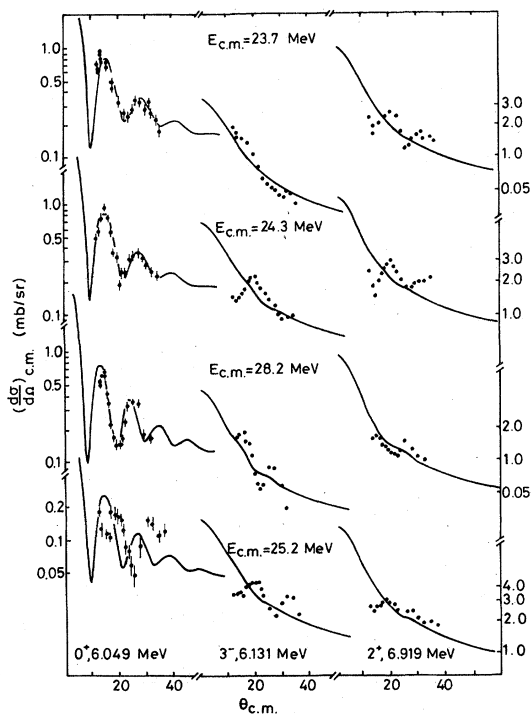


FIG. 7. The angular distributions for the 0^+ , 3^- , and 2^+ states at $E_{c.m.} = 23.7$, 24.3, 25.2, and 28.2 MeV and Hauser-Feshbach calculations.

+ $^{16}\text{O}_{g.s.} + ^{12}\text{C}_{g.s.} + ^{16}\text{O}(3^-, 6.13 \text{ MeV})$, and (iii) $^{12}\text{C}_{g.s.} + ^{16}\text{O}_{g.s.} + ^{12}\text{C}_{g.s.} + ^{16}\text{O}(0^+, 6.05 \text{ MeV})$, $^{12}\text{C}_{g.s.} + ^{16}\text{O}(2^+, 6.92 \text{ MeV})$, $^{12}\text{C}_{g.s.} + ^{16}\text{O}(4^+, 10.35 \text{ MeV})$, and $^{12}\text{C}_{g.s.} + ^{16}\text{O}(6^+, 16.20 \text{ MeV})$.

The couplings are made only within each group. For simplicity in the calculation, only one aligned rotational band for each channel was taken into account in coupling of the channels.

The coupling strength in section (i) and in section (ii) is set equal to the depth of the attractive potential in the single-excitation channel multiplied by the deformation parameters of $\beta_2 = -0.1$ in section (i) and $\gamma_3 = 0.1$ in section (ii). The strengths and form factors for the coupling between channels in section (iii) are so chosen that the internal motion of the 0^+ , 6.05-MeV, 2^+ , 6.92-MeV, 4^+ , 10.35-MeV, and 6^+ , 16.20-MeV states of ^{16}O is represented by an axially symmetric rotor.

Optical parameters of the so-called shallow potential: $V = -24 \text{ MeV}$ for $^{12}\text{C}_{g.s.} + ^{16}\text{O}_{g.s.}$, and $^{12}\text{C}(2^+) + ^{16}\text{O}_{g.s.}$ and $V = -22 \text{ MeV}$ for $^{12}\text{C}_{g.s.} + ^{16}\text{O}(3^-)$ and $^{12}\text{C}_{g.s.} + ^{16}\text{O}(0^+, 2^+, 4^+, \text{ and } 6^+)$, with $r_0 = 1.25 \text{ fm}$ and $a = 0.40 \text{ fm}$, were used. In the present calculation, the imaginary part is switched off in order to enhance the coupling effects. The β parameters in the strengths of the coupling in section (iii) were adjusted to describe the data. The results are shown in Fig. 8 where the β parameters

are chosen to be $\beta_i = +0.2$ for all the 0^+ , 6.05-, 2^+ , 6.92-, 4^+ , 10.35-, and 6^+ , 16.20-MeV states.

The excitation function calculated at $\theta_{c.m.} = 166^\circ$ for the 0^+ , 6.05-MeV state shows strong peaks at $E_{c.m.} = 18.6, 20.8, 23.2, 25.6, 28.4,$ and 31.6 MeV with widths of $\sim 250, \sim 300, \sim 500, \sim 700, \sim 1200,$ and $\sim 2000 \text{ keV}$, respectively.

A sharp rise from 18 MeV to 23.2 MeV and a gradual fall from 23.2 to 34 MeV is found. However, the doublets can not be reproduced.

For the 2^+ , 6.92-MeV state, a large peak at 22.0 MeV is produced as a result of increasing both the number of outgoing coupled channels and the strengths of the couplings between the relevant channels. This large peak at $E_{c.m.} = 22.0 \text{ MeV}$ has not been reproduced by the simple double resonance model.^{5,6} The doublets with a spike and a broad peak are seen from 25 to 34 MeV and the lower sharp spikes of the doublets correspond to the peaks for the 0^+ , 6.05-MeV state from 26 to 32 MeV.

For the 3^+ , 6.13-MeV state, the groups of resonances mainly consisting of doublets are seen around 20, 22.5, 25, 27.5, 31, and 34 MeV. The out-of-phase relation of the resonant energies in the excitation functions for the 0^+ , 6.05- and 3^+ , 6.13-MeV states is well reproduced in the calculation. On the whole the energies of the resonances appear to be lower than the data, so that the bombarding energy scale has to be expanded to reproduce the general trend of the data.

VII. DISCUSSION AND CONCLUSION

We first discuss whether and to what extent the conclusions for the lower energy region (14–23 MeV) hold also from 22.7 to 37.7 MeV, and then discuss the interpretation of the intermediate-structure resonances observed.

(1) In the higher energy region investigated here, the inelastic channels also show nonstatistical resonances of a width intermediate between Ericson fluctuations ($\Gamma_{C,N} \sim 140\text{--}220 \text{ keV}$) and ion-ion potential resonances, which were calculated for the elastic scattering at $\theta_{c.m.} = 165^\circ$ by a deep potential²⁹ or by an energy-dependent shallow potential⁴ resulting in a width of 2–5 MeV. The widths of the nonstatistical resonances for the 0^+ , 6.05-MeV state range from 640 to 720 keV and for the 2^+ , 6.92-MeV state the similar widths are observed. For the 3^+ , 6.13-MeV state groups of resonances are observed with a widths of less than 1 MeV every energy interval of 3–4 MeV.

This behavior found in the lower energy region is also found in the higher energy region.

(2) The autocorrelation functions have a Lorentzian form only in the limited region of $0 \leq \epsilon < 0.5$

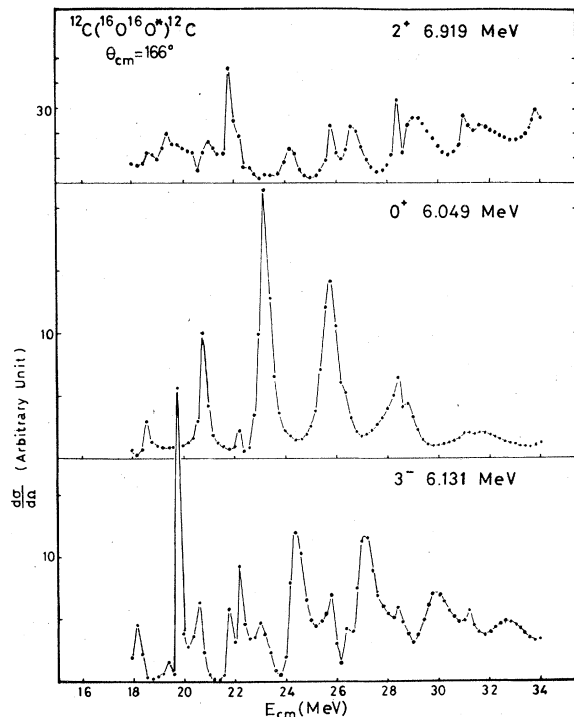


FIG. 8. The excitation functions for the 0^+ , 2^+ , and 3^- states calculated by the band-crossing model.

MeV. Thereafter, periodicities of 1.2 and 1.6 MeV appear in the autocorrelation functions of the 0^+ , 6.05-MeV state and of the 3^- , 6.13-MeV state, respectively. For the 2^+ , 6.92-MeV state the same period as for the 0^+ , 6.05-MeV state is observed. Thus this energy region seems to belong to the nonstatistical region where waves of many J values do not overlap with random phases. In other words, J narrowing occurs to enhance the yields in the excitation functions. The angular distributions show a more direct evidence for J narrowing. Although the angular range measured is experimentally limited for the 0^+ , 6.05-MeV state, single definite J values are assigned on resonances.

The oscillatory nature of the angular distributions for the 2^+ , 6.92-MeV and 3^- , 6.13-MeV states also supports J narrowing. In addition, the oscillatory features in the angular distributions for the 2^+ and 3^- states suggest that the components of $L_f = J$ and $L_f = J - 1$ are more favored than those of $L_f = J - 2$ and $L_f = J - 3$ which dominate the transmission coefficients, respectively. This fact reflects some structure of the individual resonances.

The statement that only a very few angular momenta contribute to the inelastic channels and that individual structures have a unique spin assignment still hold in the high energy region up to $E_{c.m.} = 37.7$ MeV.

(3) The main effort in the present experiment is to separate the ^{12}C particles from the reaction to the 0^+ , 6.05-MeV state from those to the 3^- , 6.13-MeV state in ^{16}O . The characteristic features appearing in the excitation function are that the sequential enhancements have the sequential total spin. Assuming that the sequential enhancements of the yield form a rotational band in the composite system of $^{12}\text{C} + ^{16}\text{O}$, the rotational band associated with the $^{12}\text{C}_{g.s.} + ^{16}\text{O}$ (0^+ , 6.05-MeV state) inelastic channel is different from that associated with the $^{12}\text{C}_{g.s.} + ^{16}\text{O}$ (3^- , 6.13-MeV state) inelastic channel.¹⁵

This reveals itself in the analysis of the Ericson's fluctuation theory; i.e., the autocorrelation function for the 0^+ , 6.05-MeV state has a periodicity of 1.2 MeV, while that for the 3^- , 6.13-MeV state has a different periodicity of 1.6 MeV. The cross-correlation function and its coefficient between the 0^+ , 6.05- and 3^- , 6.13-MeV states are out-of-phase and negative.

A comparison of the ratio of the differential cross sections predicted by the Hauser-Feshbach theory with the data is made between the excitation function for the 0^+ , 6.05-MeV and 3^- , 6.13-MeV states. The results indicate that for the 0^+ state, the averaged experimental cross section is larger, while that for the 3^- state is smaller in the energy region investigated here.

These facts indicate that at excitation energies of 40–50 MeV in ^{28}Si , the band associated with the decay to the 0^+ excited state in ^{16}O has a completely different character from the band associated with the decay to the 3^- state in ^{16}O .

(4) It is considered that the 2^+ , 6.92-MeV state in ^{16}O belongs to a member of the deformed rotational band based on the 0^+ , 6.05-MeV state. The population of the 2^+ , 6.92-MeV state is enhanced in the $^{12}\text{C}(^{16}\text{O}, ^{12}\text{C})^{16}\text{O}^*$ reaction as much as the 0^+ , 6.05-MeV state in the present energy region, and the differential cross sections are comparable to those predicted by the Hauser-Feshbach theory. The autocorrelation for the 2^+ , 6.92-MeV state is similar to that for the 0^+ , 6.05-MeV state, though the amplitude is damped for the larger value of ϵ .

The cross-correlation function between the 2^+ and 0^+ states shows a fairly strong correlation and its coefficient is positive at $\epsilon = 0$. The cross-correlation function between the 2^+ and 3^- states shows an anticorrelation and its coefficient is negative at $\epsilon = 0$ just as between the 0^+ and 3^- states. These facts support the statement that the rotational band associated with the $^{12}\text{C}_{g.s.} + ^{16}\text{O}$ (2^+ , 6.92-MeV state) is the same one associated with the $^{12}\text{C}_{g.s.} + ^{16}\text{O}$ (0^+ , 6.05-MeV state).

(5) The correspondence of the enhanced peaks in the excitation functions are not usually obtained in the weakly coupled or uncoupled calculations of the potential model as observed in the excitation functions for the 0^+ and 3^- states in ^{16}O . In order to obtain a good matching of the resonance peaks for the different channels in the band-crossing model, strong coupling is essential between close-spaced bands in the band diagram.³¹ The bands associated with the 0^+ , 6.05- and 2^+ , 6.92-MeV states are parallel in the present range of excitation energies. However, the correspondence of resonance peaks in the excitation functions was not obtained in the simple coupled channel calculation. Thus, the observation of the strong correspondence between peaks for the 0^+ and 2^+ states in the deviation functions suggests that there may exist eigenstates with the same configuration in ^{28}Si decaying to the correlated states of the 0^+ , 6.05- and 2^+ , 6.92-MeV states in the same rotational band in ^{16}O .

In addition, the fact that the width of the band for the 0^+ , 6.05-MeV state does not increase rapidly as a function of the bombarding energy suggests that the band observed in the excitation function for the 0^+ , 6.05-MeV state corresponds to the eigenstates in ^{28}Si and that they are populated during the kinematically favored collision in the $E_{c.m.} = 20$ to 33 MeV energy region. On the contrary, the state-independent potential model predicts a rapid increase of the width as a function of the bombarding

energy as shown in Fig. 8.

Thus, taking into account all statements from (1) to (5), the alpha-particle doorway state model can be accepted as the most favorable interpretation of the resonances observed in the reaction to the 0^+ , 6.05-MeV state of ^{16}O .

(6) As a further support for the formation of the alpha-particle doorway state, the value of the moment of inertia is noteworthy for the band consisting of the ground state in ^{12}C and the 0^+ , 6.05-MeV state in ^{16}O . The A parameters ($A = \hbar^2/2\mathcal{I}$) of 113 and 123 keV are obtained for the doublet.¹⁵ The grazing radius of $R_0 = 1.33(A_1^{1/3} + A_2^{1/3})$ fm, which corresponds to 74 keV in the A parameter, is extracted from the fusion data³² which bring the incident channel information in the $^{12}\text{C}_{g.s.} + ^{16}\text{O}_{g.s.}$ system. The A parameter of 113 keV gives the small value of $R_0 = 1.08 (A_1^{1/3} + A_2^{1/3})$ fm in the $^{12}\text{C}_{g.s.} + ^{16}\text{O}_{g.s.}$ system. If one takes the grazing radius in the $^{12}\text{C}_{g.s.} + ^{12}\text{C}_{g.s.}$ system, the value is found to be $R_0 = 1.20 (A_1^{1/3} + A_2^{1/3})$ fm. This value is still smaller than that for the ground states in the ^{16}O and ^{12}C system. Then, a preferable picture is that an alpha particle crystalizes outside the ^{12}C core in ^{16}O , with the excitation energy of 6.05 MeV and with $L = 0^+$, and the alpha particle is bound in the common field formed by two attached ^{12}C cores. Thus, an A parameter larger than that in $^{12}\text{C}_{g.s.} + ^{12}\text{C}_{g.s.}$ may be explicable by the smaller moment of inertia. This picture is similar to that for the alpha exchange model proposed by Michaud and Vogt,⁹ Stockstad *et al.*,^{10,11} and Brady *et al.*¹² However, this picture does not mean directly the idea of the linear chain configuration of $^{12}\text{C}-\alpha-^{12}\text{C}$ proposed by Horiuchi, Ikeda, and Suzuki,¹⁴ where the moment of inertia is expected to be larger.

In conclusion, the enhancements with definite spin and intermediate-resonance width observed in

the excitation function for the 0^+ , 6.05-MeV and 2^+ , 6.92-MeV states indicate that the sequence of these enhancements corresponds to eigenstates in ^{28}Si which are populated during the collision, have a life longer than the resonances formed in the ion-ion potential, and decay preferentially into the $^{12}\text{C} + ^{16}\text{O}^*$ (0^+ , 6.05-MeV, 2^+ , 6.92-MeV) channel. These states are similar to those proposed as alpha-particle doorway states.

On the other hand, the enhancements observed in the excitation function for the 3^- , 6.13-MeV state indicate that these enhancements may be due to the coupling between two bands formed in the potentials for the incident and exit channels, respectively. Thus, the sequence of the enhancements for the 0^+ , 6.05-MeV state of ^{16}O observed in the present work can be regarded as one of experimental evidences for the existence of the alpha-particle doorway states at excitation energies between 39.4 and 49.7 MeV in ^{28}Si .

ACKNOWLEDGMENTS

The authors are indebted to Professor J. Sanada and Professor T. Mikumo for encouragement throughout this work. They thank Professor Y. Abe and Dr. T. Matsuse for their stimulating discussions and for allowing us to use the band-crossing model code. They also thank Dr. J. J. Kolata and Dr. J. L. Quebert for the communication of their data before publication. The authors thank Professor G. C. Morrison and Professor P. E. Hodgson for giving us many valuable comments and for a critical reading of the manuscript. They are greatly indebted to the crew of Tandem Accelerator Center for fine operation of the machine. This work is partly supported by Nuclear and Solid-State Physics Project at the University of Tsukuba.

¹R. E. Malmin, R. H. Siemssen, D. A. Sink, and P. P. Singh, Phys. Rev. Lett. **28**, 1590 (1972).

²See, e.g., D. A. Bromely, in *Proceedings of the Second International Conference on Clustering Phenomena in Nuclei, College Park, Maryland, 1975*, edited by D. A. Goldberg, J. B. Marion, and S. J. Wallace, ERDA Report No. ORO-4856-26 (National Technical Information Service, Springfield, Virginia, 1975); R. H. Siemssen, in *Proceedings of the INS-IPCR Symposium on Cluster Structure of Nuclei and Transfer Reactions Induced by Heavy Ions, Tokyo, 1975*, edited by H. Kamitsubo, I. Kohno, and T. Marumori (The Institute of Physical and Chemical Research, Wako-shi, Saitama, Japan, 1975); J. Gastebois, in *Nuclear Molecular Phenomena*, edited by N. Cindro (North-Holland, Amsterdam, 1978),

p. 61, and references therein; P. Taras, in *Proceedings of the Third International Conference on Clustering Aspects of Nuclear Structure and Nuclear Reactions, Winnipeg, 1978*, edited by W. T. H. Van Oers, J. P. Svenne, J. S. C. McKee, and W. R. Falk (American Institute of Physics, New York, 1979), p. 234.

³H. Feshbach, J. Phys. (Paris) Colloq. **37**, C5-117 (1976).

⁴R. E. Malmin, J. W. Harris, and P. Paul, Phys. Rev. **C18**, 163 (1978).

⁵B. Imanishi, Phys. Lett. **27B**, 267 (1968); Nucl. Phys. **A125**, 33 (1969).

⁶W. Scheid, W. Greiner, and R. Lemmer, Phys. Rev. Lett. **25**, 176 (1970); F. J. Fink, W. Scheid, and W. Greiner, Nucl. Phys. **A118**, 259 (1972).

- ⁷Y. Abe, in *Proceedings of the Conference on Clustering Phenomena in Nuclei, University of Maryland, College Park, 1975*, (see Ref. 2), p. 500; in *Nuclear Molecular Phenomena*, edited by N. Cindro (North-Holland, Amsterdam, 1978), p. 211.
- ⁸D. Baye and P. H. Heenen, Nucl. Phys. A125, 33 (1969); D. Baye, P. H. Heenen, and M. Libert-Heineman, *ibid.* A308, 229 (1978).
- ⁹G. Michaud and E. W. Vogt, Phys. Lett. 30B, 85 (1969); Phys. Rev. C 5, 350 (1972).
- ¹⁰R. G. Stokstad, D. Shapira, L. Chua, P. Parker, M. W. Sachs, R. Wieland, and D. A. Bromley, Phys. Rev. Lett. 28, 1523 (1972).
- ¹¹D. Shapira, R. G. Stokstad, M. W. Sachs, A. Gobbi, and D. A. Bromley, Phys. Rev. C 12, 1907 (1975).
- ¹²F. P. Brady, D. A. Viggars, T. W. Conlon, and D. J. Parker, Phys. Rev. Lett. 39, 870 (1977).
- ¹³Y. Suzuki, Prog. Theor. Phys. 55, 1751 (1976); 56, 111 (1976); D. Kurath and I. S. Towner, Nucl. Phys. A222, 1 (1974).
- ¹⁴H. Horiuchi, K. Ikeda, and Y. Suzuki, Suppl. Prog. Theor. Phys. 52, 89 (1972).
- ¹⁵K. Katori, K. Furuno, and T. Ooi, Phys. Rev. Lett. 40, 1489 (1978); 41, 138(E) (1978); in *Proceedings of the International Pre-Symposium on Clustering Phenomena in Nuclei*, Tokyo, 1977, p. 82.
- ¹⁶J. Sanada, S. Seki, T. Ishihara, Y. Nagashima, T. Mikumo, M. Yamanouchi, K. Katori, K. Kuriyama, K. Furuno, and T. Aoki, Rev. Phys. Appl. 12, 1340 (1977).
- ¹⁷J. E. Spencer and H. A. Enge, Nucl. Instrum. Methods 49, 181 (1976).
- ¹⁸D. Shapira, R. M. DeVries, M. R. Clover, R. N. Boyd, and R. N. Cherry, Jr., Phys. Rev. Lett. 40, 371 (1978).
- ¹⁹R. E. Malmi, F. Kahn, and P. Paul, Phys. Rev. C 17, 2097 (1978).
- ²⁰F. Ajzenberg-Selove, Nucl. Phys. A281, 1 (1977), Table 16.9.
- ²¹P. T. Debevec, H. T. Fortune, R. E. Segel, and J. F. Tonn, Phys. Rev. C 9, 2451 (1974).
- ²²T. Ericson, Ann. Phys. (N.Y.) 23, 390 (1963).
- ²³G. Pappalardo, Phys. Lett. 13, 320 (1964).
- ²⁴J. S. Bendat and A. G. Piersol, *Random Data: Analysis and Measurement Procedures* (Wiley, New York, 1971).
- ²⁵J. J. Kolata, R. M. Freeman, F. Haas, B. Heusch, and A. Gallmann, Phys. Rev. C 19, 408 (1979).
- ²⁶W. Hauser and H. Feshbach, Phys. Rev. 87, 366 (1952).
- ²⁷L. R. Greenwood, K. Katori, R. E. Malmi, T. H. Braid, J. C. Stoltzfus, and R. H. Siemssen, Phys. Rev. C 6, 2112 (1972).
- ²⁸K. A. Eberhard, P. von Brentano, M. Boening, and R. O. Stephen, Nucl. Phys. A125, 673 (1969).
- ²⁹H. H. Gutbrod, R. Bock, W. von Oertzen, U. C. Schlotthauer-Voos, Z. Phys. 262, 377 (1973).
- ³⁰K. Furuno, K. Katori, T. Aoki, T. Ooi, and J. Sanada, J. Phys. Soc. Jpn. 44, 249 (1978); Nucl. Phys. A321, 250 (1979).
- ³¹T. Matsuse, Y. Kondo, and Y. Abe, Prog. Theor. Phys. 59, 1904 (1978).
- ³²H. Fröhlich, P. Dück, W. Galster, W. Treu, H. Voit, H. Witt, W. Kühn, and S. M. Lee, Phys. Lett. 64B, 408 (1976).